processes

MDPI

Article

A New Methodology for Film Preparation: Comparison Between Doctor Blading and Airbrushing Methods on Scaffold Materials

Hagata Emmanuely Slusarski Fonseca [1], Gideã Taques Tractz [2,*], Ana Paula Peron [2], Wesley Kordiak [1], Maria Vitória França Corrêa [1], Maico Taras da Cunha [1] and Everson do Prado Banczek [1]

[1] Campus Cedeteg, Universidade Estadual do Centro Oeste, Alameda Elio Dalla Vechia 838, Vila Carli, Guarapuava 85040-167, PR, Brazil; slusarskih@gmail.com (H.E.S.F.); wesleykordiak@gmail.com (W.K.); vihfc21@gmail.com (M.V.F.C.); mcunha@unicentro.br (M.T.d.C.); ebanczek@unicentro.br (E.d.P.B.)

[2] Campus Campo Mourão, Universidade Tecnológica Federal do Paraná, Via Rosalina Maria dos Santos, 1233, Vila Carolo, Campo Mourão 87301-899, PR, Brazil; anaperon@utfpr.edu.br

* Correspondence: gide.tractz@hotmail.com

Abstract

This paper explores the potential of the airbrushing method as a novel and cost-effective method for producing uniform titanium dioxide (TiO_2) films, crucial for enhancing the efficiency of dye-sensitized solar cells. The techniques performed were SEM and EDS images, OCP curves, photochronoamperometry, j-V curves, and impedance spectroscopy. Comparative analysis with the doctor blade methodology has noted a higher uniformity compared to the AB method, with the ability to improve the charge transportation and PCE (1.987%) and reduce the recombination process in the TiO_2/electrolyte interface (τ_e = 0.012 s). Insights from EIS spectroscopy and intensity-modulated spectroscopy offer mechanistic elucidations of the enhanced performance. Overall, this study highlights airbrushing as a promising approach for advancing the development of high-performance solar energy systems.

Keywords: TiO_2; films; DSSC; semiconductor; electrochemical measurements

check for updates

Academic Editor: Davide Papurello

Received: 2 July 2025
Revised: 8 August 2025
Accepted: 10 August 2025
Published: 12 August 2025

Citation: Fonseca, H.E.S.; Tractz, G.T.; Peron, A.P.; Kordiak, W.; Corrêa, M.V.F.; da Cunha, M.T.; Banczek, E.d.P. A New Methodology for Film Preparation: Comparison Between Doctor Blading and Airbrushing Methods on Scaffold Materials. *Processes* **2025**, *13*, 2537. https://doi.org/10.3390/pr13082537

Copyright: © 2025 by the authors. Licensee MDPI, Basel, Switzerland. This article is an open access article distributed under the terms and conditions of the Creative Commons Attribution (CC BY) license (https://creativecommons.org/licenses/by/4.0/).

1. Introduction

Global warming, driven primarily by human activities, poses a significant threat to the planet, leading to rising temperatures, extreme weather events, and disruptions to ecosystems worldwide, as discussed by the IPCC (Intergovernmental Panel on Climate Change). From this perspective, the use of renewable energy such as solar panels is a promising solution for reducing the emission of pollutant gas [1].

Solar cells are devices capable of converting solar energy into electricity. Silicon-based solar devices, perovskites, and dye solar cells are some device structures that have been extensively studied in the last decade. These last two classes have presented in composition a semiconductor film under a conductive glass, able to separate the charges in such interfaces [2,3].

The semiconductor material acts as a scaffold, receiving the charge from photosensitive material generated by solar radiation [3]. Due to the trap/detrap mechanism, these electrons are transported to the counter electrode, generating a current flow and j value. In perovskite solar cells, films with thicknesses in the order of 100 nm and 20 µm for dye-sensitized solar cells (DSSC) are recommended to produce an efficient solar device [4,5].

Another key factor influencing the performance of dye-sensitized solar cells is the morphological and optical properties of the semiconductor film. The porosity, particle size,

and surface area of the TiO_2 layer directly affect dye adsorption and electron diffusion, which are critical for efficient light harvesting and charge transport [3]. Additionally, the optical transparency and light-scattering behavior of the film must be optimized to enhance photon capture within the active layer [5]. Therefore, controlling not only the thickness but also the structure of TiO_2 is essential to achieving high-performance devices, especially when employing low-cost and scalable deposition techniques.

Regarding uniform films, many methodologies are applied to enhance charge transportation and photoconversion energy efficiency. Ito and co-workers used pastes of TiO_2 containing ethyl cellulose with ethanol coated by the screen printing method, resulting in an electrode thickness of 17 μm [6]. The use of the doctor blading method, in addition to the use of an aqueous paste, can also be found in a large number of papers [1,7–9]. Film fabrication using the spin coating method has proven to be a good alternative. On the other hand, the uniformity control of these techniques is impaired, reducing the reproducibility of the methods. These discussed techniques present specific limitations: screen printing and doctor blading are low-cost and suitable for thick films but often show low resolution; spin coating provides good thickness control but is less appropriate for large-area deposition and requires precise viscosity adjustment [7–9]. Additionally, poor adhesion, film cracking during drying, and environmental sensitivity can compromise reproducibility [5].

Airbrushing deposition, using an airbrush component, stands out as one of the most promising techniques for generating large areas of cost-effective TiO_2 films simply [10]. An airbrush is a tool used for spraying various media, such as paint or ink, onto a surface. It consists of a handheld device connected to a compressor that delivers pressurized air. The airbrush allows for precise control over the application of the media, making it suitable for creating detailed artwork, film production, customizing automotive finishes, and more [11]. In the literature, its use is related to dye degradation [10], cellulose deposition [12], and also to DSSC with Ag-ZnO scaffold materials [13]; however, the use of aqueous TiO_2 paste is not found in the literature.

This paper aims to propose the use of a non-expensive and easy-to-construct airbrushing method to produce uniform films with a comparison between the doctor blading method and solar cell preparation with a complete device characterization.

2. Materials and Methods

TiO_2 paste was prepared as follows: 3 g of TiO_2 anatase purchased from Aldrich® was put in a mortar, followed by the insertion of 0.1 mL of acetylacetone, 1 mL of polyethilene glycol, 3 mL of distilled water, and 0.1 mL of triton X. The material was macerated for 30 min to produce an emulsion with a reduced size [14,15].

The paste was coated by the doctor blading standard methodology and using the airbrushing method (at an airbrush distance of 10 cm from the FTO substrate, applying a pressure of 40 pounds per square inch (psi)). Two layers of films were coated under FTO (fluorine-doped tin oxide ~7 sq^{-1} by Aldrich® (São Paulo City, SP, Brazil)) followed by calcination at 450 °C. N719 dye impregnation was carried out by immersion for 24 h of the films using both methodologies [9,16]. Films were analyzed by scanning electron microscopy, with an energy of 20 kV with EDS mapping.

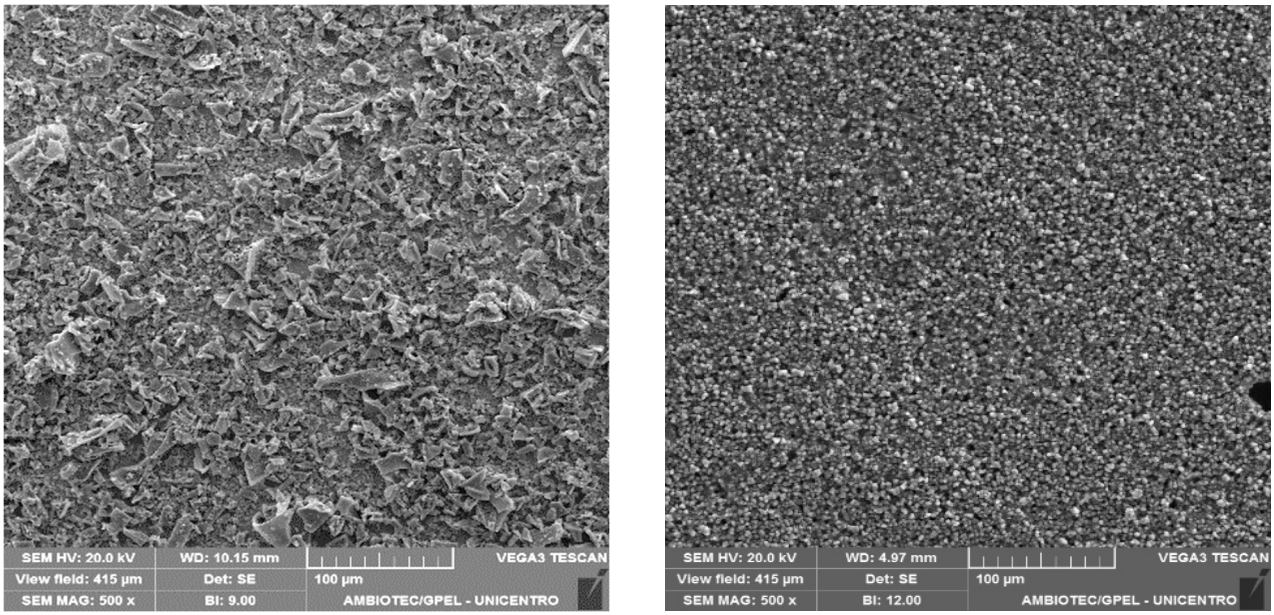
A dye solar cell was fabricated following the previously outlined procedure, employing the photoanode. A Pt counter electrode was synthesized via cyclic voltammetry, and an electrolyte solution consisting of 0.5 mol L^{-1} tert-butylpyridine, 0.6 mol L^{-1} tetrabutylammonium iodide, 0.1 mol L^{-1} lithium iodide, and 0.2 mol L^{-1} resublimed iodide dissolved in methoxypropionitrile was utilized, within an active area of 0.2 cm^{-2}.

J-V curves, open circuit potential, and photochronoamperometric curves were conducted under illumination with an AM 1.5 G using a light intensity of 100 mA cm^{-2}. These ex-

periments were carried out utilizing a Zennium Zahner® potentiostat (Kronach, Germany) equipped with a solar simulator featuring a xenon lamp. Electrochemical impedance spectroscopy was performed over a range of 10 mHz to 10 kHz with an amplitude of 10 mV. Intensity-modulated photovoltage spectroscopy (IMVS) and intensity-modulated photocurrent spectroscopy (IMPS) were executed within a frequency range of 100 mHz to 1 kHz.

3. Results and Discussion

In Figure 1, the SEM images of the TiO_2 films prepared by doctor blading and airbrushing methods (AB) are depicted.



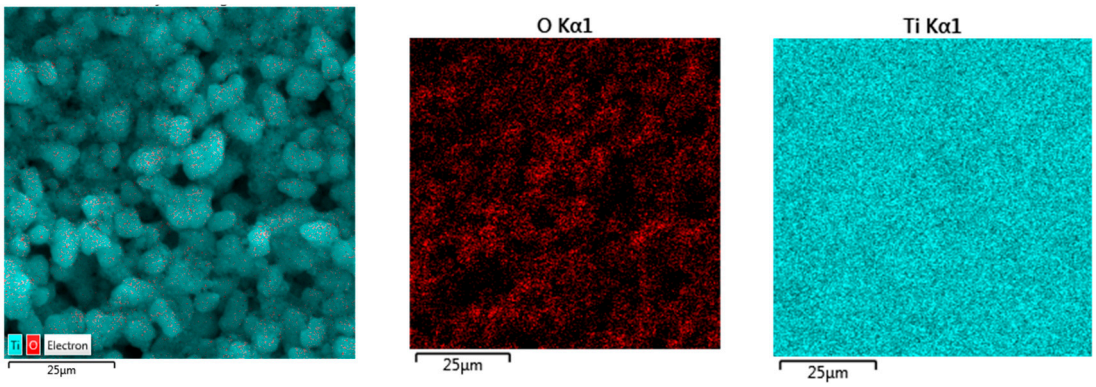
(**a**) (**b**)

Figure 1. SEM images of FTO with TiO_2 coated by (**a**) doctor blading and (**b**) airbrushing methods.

The analysis of the micrographs demonstrates that the deposited TiO_2 exhibits dissimilar morphologies depending on the deposition methods. It is possible to observe that the sample prepared by doctor blading presents an irregular morphology with clusters of various morphologies and dimensions. For the TiO_2-coated sample using airbrushing, it was possible to observe that the morphology is more regular without the formation of clusters and particles with rounded shapes, which may suggest a more efficient interaction with the sensitizing dye [17]. It is worth noting that the TiO_2 films deposited by airbrushing exhibit nanopores on their surface. The presence of such nanoporosity may contribute to a more compact electrical double layer at the TiO_2/electrolyte interface, facilitating improved charge transfer in this region and consequently enhancing the photoelectrochemical parameters of the cell [5].

It is important to note that the airbrushing technique allows for a wide range of film thicknesses depending on the operational parameters, such as the airbrush pressure and the distance between the nozzle and the substrate. These parameters can be adjusted to control the morphology and thickness of the deposited TiO_2 films, as described above. Due to this variability and the ability to fine-tune the deposition process, direct thickness measurements were not performed for the airbrushed films in this study. In contrast, films produced by the doctor blading method exhibited thicknesses around 20 µm, as measured by SEM microscopy [18]. This approach ensured a more reproducible film thickness for the doctor blading samples while maintaining flexibility in the airbrushing process.

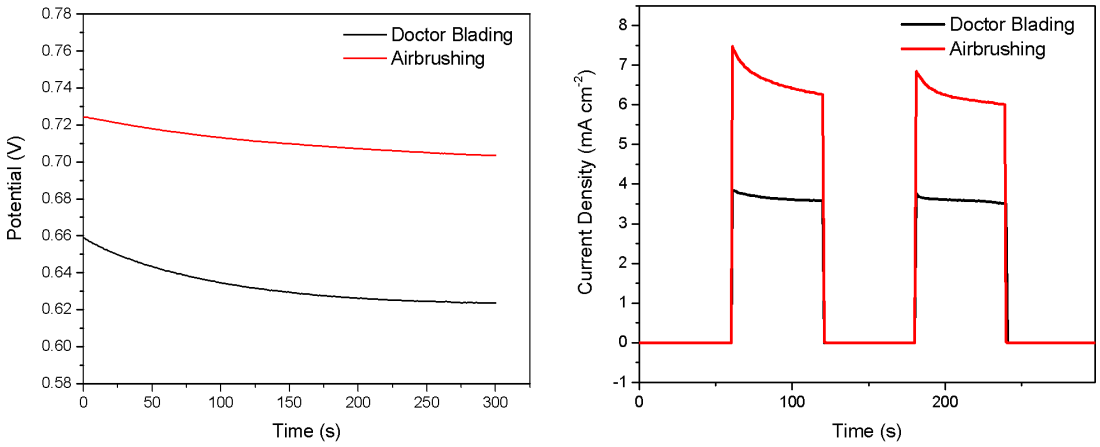
The elemental composition of the TiO_2 films deposited by the AB method was determined by energy-dispersive spectroscopy, and the results are presented in Figure 2. The analysis of the results demonstrates that the composition of the titanium film did not exhibit impurities of chemical elements that could influence the photovoltaic response of the films. Titanium and oxygen elements were detected, suggesting that the TiO_2 coating was formed. Additionally, it is observable that the composition of the films is homogeneous, as the distribution of oxygen and titanium elements is spread across the entire surface, as observed in the mapping images obtained in Figure 2.



(**a**) (**b**) (**c**)

Figure 2. EDS mapping of TiO_2 films produced by airbrushing method: (**a**) Ti and O, (**b**) oxygen distribution, and (**c**) titanium.

Open circuit potential (Voc) analysis and photochronoamperometric curves of the dye solar devices are depicted in Figure 3a,b, respectively.



(**a**) (**b**)

Figure 3. Open circuit potential analysis (**a**) and photochronoamperometric curves (**b**) of the dye solar devices.

A higher stable potential (V = 0.72 V) for dye cells produced by the AB method was observed when compared to the doctor blading methodology (V = 0.63 V). It is known that the V_{OC} formation is characterized by the difference between the Fermi level (E_F) of the semiconductor device and the E_{redox} of the electrolyte. However, the dye anchored in the scaffold surface may shift the E_F, producing different values depending on the surface film's properties. A similar behavior of V_{OC} variation by film modification can be observed in several papers [19–21].

As verified in SEM images, the formation of a highly uniform film and also the higher porosity indicated by the color of the films shifted the E_F level, generating more significant

V values [5,22,23]. As a consequence, the j values also must be influenced, and to verify this significant parameter, the photochronoamperometric curves are analyzed in Figure 3b.

The solar cell behavior was observed in both samples since there was a current flowing when the light was turned on. Figure 3b also indicates the capability of the airbrushing method to generate higher J values in dye solar cells, with ~6 mA cm^{-2} being found. Such behavior may be due to the high uniformity of the film and porosity, enhancing the anchored surface dye, and the possibility of a higher charge injected in the scaffold material [5,24,25]. Extended stability tests were not conducted in this study; however, the literature consistently demonstrates the long-term robustness of systems based on TiO_2 photoanodes sensitized with ruthenium-based dyes. Previous reports show that such systems can retain more than 90% of their initial photocurrent over a period of two months under continuous illumination. Moreover, according to Grätzel and co-workers, these devices can endure at least five million redox turnovers without decomposition, highlighting the exceptional durability of DSSCs employing this configuration [2].

To analyze the photoconversion energy efficiency (PCE), J-V measurements were performed, and the results are available in Figure 4 and Table 1.

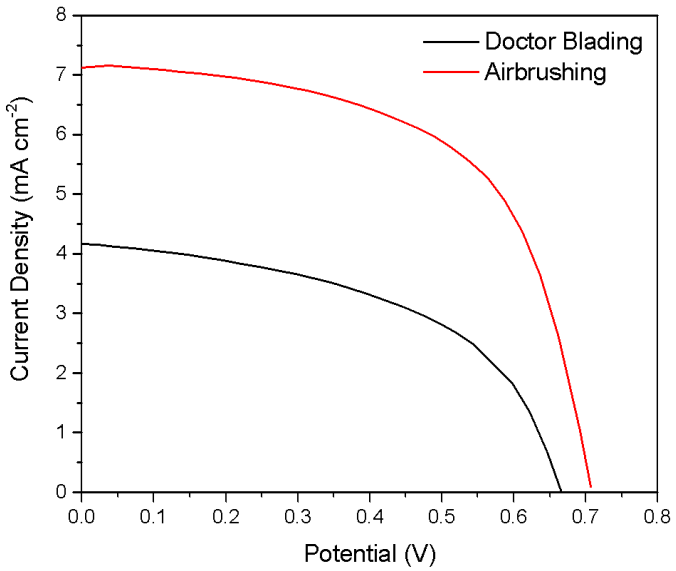


Figure 4. J-V curves of DSSC produced by airbrushing and doctor blading methodologies.

Table 1. Photovoltaic parameters of DSSC produced using both doctor blading and airbrushing methodologies.

Deposition Method	V (V)	J (mA cm^{-2})	FF	PCE (%)
Doctor blading	0.696 ± 0.027	3.42 ± 1.04	0.430 ± 0.110	1.023 ± 0.254
Airbrushing	0.641 ± 0.090	6.09 ± 1.19	0.509 ± 0.116	1.987 ± 0.640

Photoconversion energy efficiency (*PCE*) was calculated using Equation (1), with j_{sc} representing the short current density values, V_{oc} the open circuit potential, *FF* the fill factor, and P_{in} the incident light of 100 mW cm^{-2} [26].

$$PCE = \frac{j_{sc} V_{oc} FF}{P_{in}} \times 100\% \quad (1)$$

In Table 1, a superior capability of the airbrushing method to produce a higher efficiency solar device is observed, since airbrushing resulted in *PCE* = 1.987 ± 0.640% while the standard doctor blade films generate *PCE* = 1.023 ± 0.254%.

It is also known that the trap/detrap mechanism governs the transport mechanism in such devices. Since light strikes the device, the charges generated do not move freely to the conduction band edge but are trapped in some energy states above the conduction band edge (BC). Some conditions of uniformity, such as the crystallinity of the film, must influence this mechanism and produce different current values. The cell with TiO_2 obtained by airbrushing exhibited efficiency values 2.03 times higher than the electrode deposited by doctor blading. This novel methodology demonstrates the viability for the production of efficient solar systems. The facile adaptability of thickness control renders it suitable for the production of electron transport materials on FTO substrates and their application in other systems, such as perovskite solar cells, thereby presenting a promising alternative to spin coating utilization [26–30].

Electrochemical impedance spectroscopy was performed to analyze the charge transfer process in cell interfaces and the results are depicted in Figure 5.

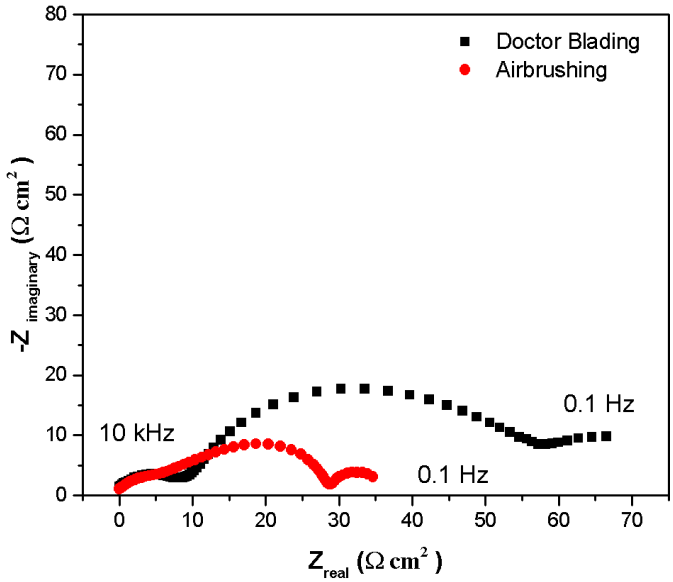


Figure 5. EIS Nyquist diagram of DSSC produced by airbrushing and doctor blading methodologies.

As demonstrated by Guimaraes and co-workers [4], in a Nyquist diagram, the first semicircle at higher frequencies is characterized by the Pt/electrolyte interface, while the second arc, at intermediate frequencies, is indicated by the TiO_2, dye/electrolyte interface. At lower frequencies, 0.1 Hz, the cell is governed by the diffusional process of I^-/I_3^- ions [31,32].

For such systems, a lower resistance to the intermediate semicircle of airbrushing films is noted, indicating a reduced resistance of charge transport in the scaffold material. As a result of the uniform and well-distributed TiO_2 particles on the FTO surface (Figure 1) of airbrushing films, electrons from the dye could be better transported to the Pt counter electrode, improving the current and consequently the PCE values, showing again that such a deposition methodology is a suitable tool for efficient film production.

In Figure 6, the Bode diagram for the studied systems is presented. In this figure, three time constants can be observed, with the first one evident at high frequencies around 1000 Hz, associated with charge transfer processes at the counter-electrode surface. The second time constant was observed at frequencies around 1 Hz and is related to transport processes at the oxide/dye/electrolyte interface. At low frequencies, around 100 mHz, the third time constant can be observed, corresponding to the diffusion of triiodide ions in the electrolytic solution. Although the three time constants were evidenced for both samples, a displacement concerning the phase angle and frequency was observed.

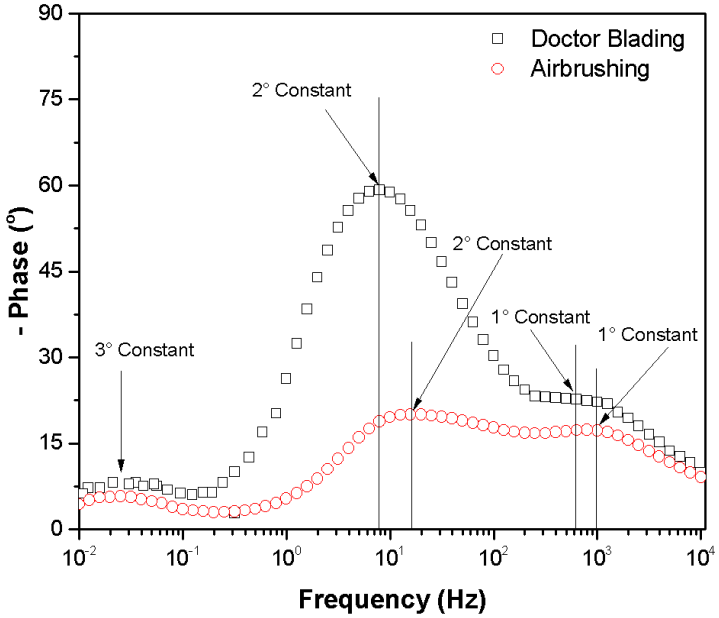


Figure 6. EIS Bode diagram for DSSC produced by airbrushing and doctor blading methodologies.

The smaller phase angles measured for the solar cells with TiO_2 electrodes obtained by airbrushing indicate that the electrical resistance needed for the processes to occur is lower, suggesting higher conductivity and a more efficient system [33–35]. The displacement of the first and second time constants to higher frequencies indicates a shorter response time for each process associated with these constants, suggesting that the charge transfer and transport processes at the oxide/dye/electrolyte interface are faster for the airbrushed cell.

It is also known that the most significant reactions in DSSC are collection (Reaction 1) and recombination (2), and a key for a competitive device is the 2 suppression and 1 improvement.

$$TiO_2\ (e^-) + Pt \rightarrow TiO_2 + Pt\ (e^-) \quad \text{(Reaction 1)}$$

$$TiO_2\ (e^-) + Electrolyte^+ \rightarrow TiO_2 + Electrolyte \quad \text{(Reaction 2)}$$

As EIS does not allow the separation of Reactions 1 and 2, IMVS and IMPS were performed in short circuit conditions and open circuit potential, respectively, in Figure 7. Collection time and recombination time were determined using Equations (2) and (3).

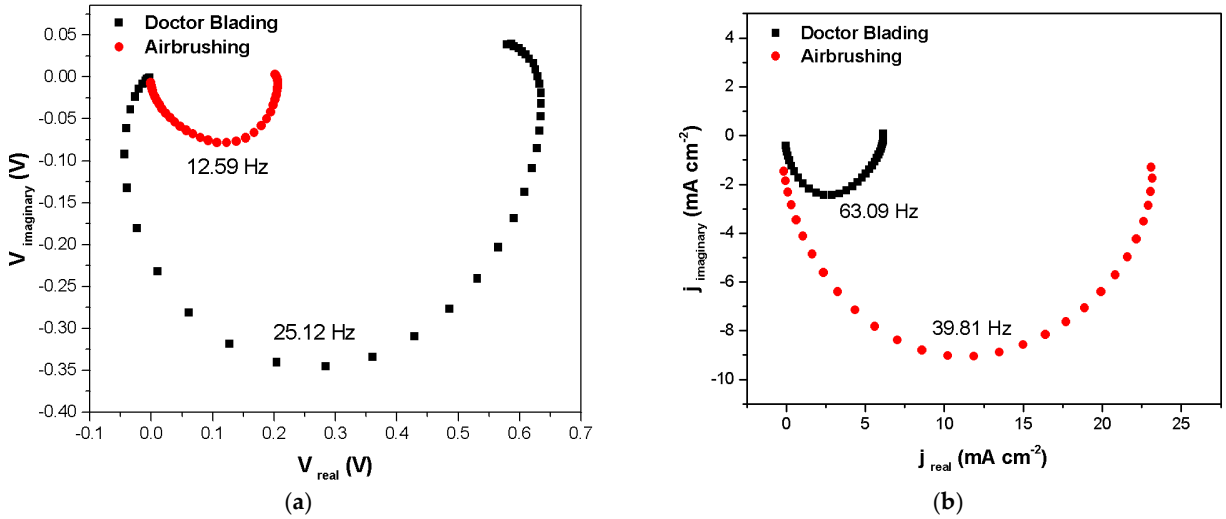


Figure 7. IMVS (**a**) and IMPS (**b**) of DSSC produced by airbrushing and doctor blading methodologies.

$$\mathfrak{t}_e = \frac{1}{2\pi f_{min}} \quad (2)$$

$$\mathfrak{t}_c = \frac{1}{2\pi f_{min}} \quad (3)$$

When the light strikes the device, the electron from the dye HOMO state is excited for the LUMO state, being injected to BC of TiO_2. These electrons could be transported to the external circuit, in the Pt electrode, generating a current flow (Reaction; $\mathfrak{t}_c$), or they could react with an oxidized electrolyte (Reaction 2; $\mathfrak{t}_e$), making the electron flow $\mathfrak{t}$e impossible.

For cell analysis, $\mathfrak{t}_e$ = 0.012 s was verified for the airbrushing method, while $\mathfrak{t}_e$ = 0.006 for standard doctor blading, suggesting that the AB method has been able to reduce the recombination rate due to the lower resistance (EIS Spectra), improving the PCE value of the device.

Regarding IMPS analysis, a frequency shift to smaller values was noted for the airbrushing method, indicating a superior collection time for the AB methodology of film preparation ($\mathfrak{t}_c$ = 0.0039 s). This interesting behavior was also observed for the use of doped materials, characteristic of the existence of new energy states created above the conduction band edge [1]. As such, it is coherent to suggest that the airbrushing method, due to uniformity, size distribution, and dye-anchored concentration, could influence such substrates, reducing both transport and recombination reactions (as also demonstrated by the J-V dark measurement, in the Supplementary Materials, due to lower leakage currents). However, the electron amount was positively influenced by the new technique, causing an increase in PCE value, as seen in Table 1.

Additionally, the presence of new energy states increases the collection time, consequently resulting in an increase in the diffusion process in the solar cell, characterized by the decay in current density observed in the photocurrent curve in Figure 3b [35]. The diffusional behavior, within a limit, is necessary for the functioning of the solar cell, and for the cell prepared by airbrushing, diffusion improved the solar cell response, as observed in the electrochemical tests and efficiency determination of the cell.

Although the airbrushing technique demonstrated promising results for TiO_2 film deposition in photovoltaic applications, several avenues remain open for further investigation. Future research could explore the long-term operational stability of the devices under continuous illumination and thermal stress. Additionally, the optimization of airbrushing parameters, such as nozzle–substrate distance, solvent system, and multi-layer strategies, could enhance film reproducibility and performance. The integration of dopants or composite materials (e.g., graphene or metal oxides) into the TiO_2 paste may also improve electron mobility and light scattering. Furthermore, the scalability of this method for flexible or tandem solar cells remains a promising direction for applied studies.

4. Conclusions

The solar cells prepared with TiO_2 deposited by airbrushing exhibited superior results compared to the cells deposited by doctor blading. The higher efficiency measured for the airbrushed solar cell is attributed to the homogeneous morphology of the TiO_2 layer, as determined by scanning electron microscopy. The results of energy-dispersive spectroscopy demonstrated that the deposited layer is composed of titanium and oxygen, which are evenly distributed throughout the sample. The homogeneity of morphology and composition promoted greater efficiency of the airbrushed cell.

Electrochemical results confirmed that the airbrushed cell is more efficient (with PCE = 1.987), as higher electric potential values, lower impedances, higher current densities, and shorter electronic injection times were determined. The collection time for the

airbrushed cell was longer than for the doctor blading cell; however, with a longer residence time of electrons in the titanium oxide, there is an increase in electrolyte diffusion. This diffusion is necessary for the functioning of the photovoltaic system.

Supplementary Materials: The following supporting information can be downloaded at: https://www.mdpi.com/article/10.3390/pr13082537/s1, Figure S1: J-V dark curves to DSSC produced by Airbrushing and Doctor Blading methodology.

Author Contributions: H.E.S.F.: conceptualization, methodology, writing—original draft preparation; G.T.T.: conceptualization, methodology, validation; A.P.P.: formal analysis, conceptualization, data curation; W.K.: conceptualization, methodology, data curation, software; M.V.F.C.: investigation, methodology; M.T.d.C.: project administration, investigation, formal analysis; E.d.P.B.: project administration, writing—original draft preparation, writing—original draft preparation. All authors have read and agreed to the published version of the manuscript.

Funding: This research received no external funding.

Data Availability Statement: The original contributions presented in this study are included in the article/Supplementary Material. Further inquiries can be directed to the corresponding author.

Conflicts of Interest: The authors declare no conflicts of interest.

Abbreviations

The following abbreviations are used in this manuscript:

AB	Airbrushing
DSSC	Dye-Sensitized Solar Cells
EDS	Energy-Dispersive X-ray Spectroscopy
EIS	Electrochemical Impedance Spectroscopy
FTO	Fluorine-Doped Tin Oxide
IMPS	Intensity-Modulated Photocurrent Spectroscopy
IMVS	Intensity-Modulated Photovoltage Spectroscopy
IPCC	Intergovernmental Panel on Climate Change
OCP	Open-Circuit Potential
SEM	Scanning Electron Microscopy
BC	Conduction Band Edge
PCE	Photoconversion Energy Efficiency

References

1. Tractz, T.; Regina, S.; Antunes, M.; Rog, P. Nb/TiO_2 oxides: A study of synthesis and electron transport mechanism as an ETL in a solar device. *J. Photochem. Photobiol. A Chem.* **2023**, *444*, 114899. [CrossRef]
2. O'Regan, B.; Grätzel, M. A low-cost, high-efficiency solar cell based on dye-sensitized colloidal TiO_2 films. *Nature* **1991**, *353*, 737–740. [CrossRef]
3. Grätzel, M. Photoelectrochemical cells. *Nature* **2001**, *414*, 338–344. [CrossRef]
4. Guimarães, R.R.; Parussulo, A.L.A.; Toma, H.E.; Araki, K. Enlightening the synergic effect of anatase/rutile mixtures in solar cells. *Electrochim. Acta* **2016**, *188*, 523–528. [CrossRef]
5. Hagfeldt, A.; Boschloo, G.; Sun, L.; Kloo, L.; Pettersson, H. Dye-Sensitized Solar Cells. *Chem. Rev.* **2010**, *110*, 6595–6663. [CrossRef]
6. Ito, S.; Chen, P.; Comte, P.; Nazeeruddin, M.K.; Liska, P.; Gra, M. Fabrication of Screen-Printing Pastes From TiO_2 Powders for Dye-Sensitised Solar Cells. *Prog. Photovolt. Res. Appl.* **2007**, *15*, 603–612. [CrossRef]
7. Tractz, T.; Paula, A.; Matheus, C.; Fernanda, L.; Larsson, G.; Rodrigues, P. The use of 2-Mercaptobenzothiazole as a new co-adsorbent in dye-sensitized solar cells. *Opt. Mater.* **2022**, *131*, 112658. [CrossRef]
8. Kumar, M.H.; Yantara, N.; Dharani, S.; Graetzel, M.; Mhaisalkar, S.; Mathews, N. Flexible, low-temperature, solution processed ZnO-based perovskite solar cells using doctor-blading. *Energy Environ. Sci.* **2013**, *6*, 3439–3445. [CrossRef]

9. Tractz, G.T.; Viomar, A.; Dias, B.V.; De Lima, C.A.; Banczek, E.P.; Da Cunha, M.T.; Antunes, S.R.M.; Rodrigues, P.R.P. Recombination study of dye sensitized solar cells with natural extracts. *J. Braz. Chem. Soc.* **2019**, *30*, 371–378. [CrossRef]
10. Nguyen-phan, T.; Hung, V.; Viet, T.; Hong, S.; Jung, E. Fabrication of TiO_2 nanostructured fi lms by spray deposition with high photocatalytic activity of methylene blue. *Mater. Lett.* **2010**, *64*, 1387–1390. [CrossRef]
11. Cassano, C.L.; Georgiev, T.Z.; Fan, Z.H. Using airbrushes to pattern reagents for microarrays and paper-fluidic devices. *Nat. Publ. Gr.* **2017**, *3*, 17055. [CrossRef]
12. Ohm, W.; Pandit, P.; Ko, V.; Rojas, R.; Yu, S.; Brett, C.J.; So, D.L.; Roth, S.V. Morphological properties of airbrush spray-deposited enzymatic cellulose thin films. *J. Coat. Technol. Res.* **2018**, *15*, 759–769. [CrossRef]
13. Tarwal, N.L.; Patil, V.L.; Rani, J.R.; Gurav, K.V.; Shaikh, J.S.; Khandekar, M.S.; Harale, N.S.; Patil, P.S.; Jang, J.H. Plasmonic DSSC performance of spray deposited Ag-ZnO and Au-ZnO films. *Chin. J. Phys.* **2021**, *73*, 581–588. [CrossRef]
14. Parussulo, A.L.A.; Bonacin, J.A.; Toma, S.H.; Araki, K.; Toma, H.E. Unravelling the chemical morphology of a mesoporous titanium dioxide interface by confocal Raman microscopy: New clues for improving the efficiency of dye solar cells and photocatalysts. *Langmuir* **2009**, *25*, 11269–11271. [CrossRef]
15. Tractz, G.T.; da Luz, F.S.; Antunes, S.R.M.; Banczek, E.D.P.; da Cunha, M.T.; Rodrigues, P.R.P. Nb_2O_5 synthesis and characterization by Pechini method to the application as electron transport material in a solar device. *Sol. Energy* **2021**, *216*, 1–6. [CrossRef]
16. Zhang, L.; Cole, J.M. Anchoring groups for dye-sensitized solar cells. *ACS Appl. Mater. Interfaces* **2015**, *7*, 3427–3455. [CrossRef]
17. Shikoh, A.S.; Ahmad, Z.; Touati, F.; Shakoor, R.A.; Al-Muhtaseb, S.A. Optimization of ITO glass/TiO_2 based DSSC photo-anodes through electrophoretic deposition and sintering techniques. *Ceram. Int.* **2017**, *43*, 10540–10545. [CrossRef]
18. Kumari, J.M.K.W.; Sanjeevadharshini, N.; Dissanayake, M.A.K.L.; Senadeera, G.K.R.; Thotawattahe, C.A. The effect of TiO_2 photoanode film thickness on photovoltaic properties of dye-sensitized solar cells. *Ceylon J. Sci.* **2016**, *45*, 1. [CrossRef]
19. Ismail, R.A.; Al-Diabat, M. Structural, optical and electrical properties of nanostructured TiO_2 thin films prepared by spin coaing technique for optoelectronic applications. *Ceram. Int.* **2020**, *46*, 2391–2399. [CrossRef]
20. Tractz, G.T.; Maia, G.A.R.; Dias, B.V.; Banczek, E.D.P.; Molinares, M.A.; da Cunha, M.T.; Rodrigues, P.R.P. Influence of deposition methodology and heating treatment on dye sensitized solar cell with natural extract. *Orbital Electron. J. Chem.* **2018**, *10*, 3. [CrossRef]
21. Nissfolk, J.; Fredin, K.; Hagfeldt, A.; Boschloo, G. Recombination and transport processes in dye-sensitized solar cells investigated under working conditions. *J. Phys. Chem. B* **2006**, *110*, 17715–17718. [CrossRef]
22. Correa-Baena, J.P.; Tress, W.; Domanski, K.; Anaraki, E.H.; Turren-Cruz, S.H.; Roose, B.; Boix, P.P.; Grätzel, M.; Saliba, M.; Abate, A.; et al. Identifying and suppressing interfacial recombination to achieve high open-circuit voltage in perovskite solar cells. *Energy Environ. Sci.* **2017**, *10*, 1207–1212. [CrossRef]
23. Meen, T.H.; Jhuo, Y.T.; Chao, S.M.; Lin, N.Y.; Ji, L.W.; Tsai, J.K.; Wu, T.C.; Chen, W.R.; Water, W.; Huang, C.J. Effect of TiO_2 nanotubes with $TiCl_4$ treatment on the photoelectrode of dye-sensitized solar cells. *Nanoscale Res. Lett.* **2012**, *7*, 1–5. [CrossRef]
24. Gong, J.; Sumathy, K.; Qiao, Q.; Zhou, Z. Review on dye-sensitized solar cells (DSSCs): Advanced techniques and research trends. *Renew. Sustain. Energy Rev.* **2017**, *68*, 234–246. [CrossRef]
25. Sivakumar, G.; Bertoni, A.H.; Kim, H.S.; Marchezi, P.E.; Bernardo, D.R.; Hagfeldt, A.; Grätzel, M.; Zakeeruddin, S.M.; Nogueira, A.F. Design, synthesis and characterization of 1,8-naphthalimide based fullerene derivative as electron transport material for inverted perovskite solar cells. *Synth. Met.* **2019**, *249*, 25–30. [CrossRef]
26. Chen, C.; Song, Z.; Xiao, C.; Zhao, D.; Shrestha, N.; Li, C.; Yang, G.; Yao, F.; Zheng, X.; Ellingson, R.J.; et al. Achieving a high open-circuit voltage in inverted wide-bandgap perovskite solar cells with a graded perovskite homojunction. *Nano Energy* **2019**, *61*, 141–147. [CrossRef]
27. Ding, B.; Huang, S.Y.; Chu, Q.Q.; Li, Y.; Li, C.X.; Li, C.J.; Yang, G.J. Low-temperature SnO_2-modified TiO_2 yields record efficiency for normal planar perovskite solar modules. *J. Mater. Chem. A* **2018**, *6*, 10233–10242. [CrossRef]
28. Ke, W.; Fang, G.; Wang, J.; Qin, P.; Tao, H.; Lei, H.; Liu, Q.; Dai, X.; Zhao, X. Perovskite solar cell with an efficient TiO_2 compact film. ACS Appl. *Mater. Interfaces* **2014**, *6*, 15959–15965. [CrossRef]
29. Guimaraes, R.R.; Parussulo, A.L.A.; Araki, K. Impact of nanoparticles preparation method on the synergic effect in anatase/rutile mixtures. *Electrochim. Acta* **2016**, *222*, 1378–1386. [CrossRef]
30. Guimaraes, R.R.; Parussulo, A.L.A.; Matias, T.A.; Toma, H.E.; Araki, K. Electrostatic blocking barrier as an effective strategy to inhibit electron recombination in DSSCs. *Electrochim. Acta* **2017**, *255*, 92–98. [CrossRef]
31. Fabregat-Santiago, F.; Bisquert, J.; Garcia-Belmonte, G.; Boschloo, G.; Hagfeldt, A. Influence of electrolyte in transport and recombination in dye-sensitized solar cells studied by impedance spectroscopy. *Sol. Energy Mater. Sol. Cells* **2005**, *87*, 117–131. [CrossRef]
32. Dhas, V.; Muduli, S.; Agarkar, S.; Rana, A.; Hannoyer, B.; Banerjee, R.; Ogale, S. Enhanced DSSC performance with high surface area thin anatase TiO_2 nanoleaves. *Sol. Energy* **2011**, *85*, 1213–1219. [CrossRef]
33. Tsai, C.-H.; Hsiao, Y.-C.; Chuang, P.-Y. Investigation of Electrochemically Deposited and Chemically Reduced Platinum Nanostructured Thin Films as Counter Electrodes in Dye-Sensitized Solar Cells. *Coatings* **2018**, *8*, 56. [CrossRef]

34. Bisquert, J.; Fabregat-Santiago, F. *Impedance Spectroscopy: A General Introduction and Application to Dye-Sensitized Solar Cells, Dye-Sensitized Solar Cells*; EPFL Press: Lausanne, Switzerland, 2010; p. 98.
35. Barnes, P.R.F.; Miettunen, K.; Li, X.; Anderson, A.Y.; Bessho, T.; Gratzel, M.; O'Regan, B.C. Interpretation of optoelectronic transient and charge extraction measurements in dye-sensitized solar cells. *Adv. Mater.* **2013**, *25*, 1881–1922. [CrossRef] [PubMed]

Disclaimer/Publisher's Note: The statements, opinions and data contained in all publications are solely those of the individual author(s) and contributor(s) and not of MDPI and/or the editor(s). MDPI and/or the editor(s) disclaim responsibility for any injury to people or property resulting from any ideas, methods, instructions or products referred to in the content.